Wear and friction of TiAlN/VN coatings against Al2O3 in air at room and elevated temperatures

ZHOU, Z., RAINFORTH, W. M., LUO, Q. <http://orcid.org/0000-0003-4102-2129>, HOVSEPIAN, Papken <http://orcid.org/0000-0002-1047-0407>, OJEDA, J. J. and ROMERO-GONZALEZ, M. E.

Wear and friction of TiAlN/VN coatings against Al2O3 in air at room and elevated temperatures

Z. Zhou[a], W.M. Rainforth[a], Q. Luo[b], P.Eh. Hovsepian[b], J.J. Ojeda[c], M.E. Romero-Gonzalez[d]

[a] Department of Engineering Materials, University of Sheffield, Mappin Street, Sheffield S1 3JD, UK

[b] Materials Engineering Research Institute, Sheffield Hallam University, Howard Street, Sheffield S1 1WB, UK

[c] Experimental Techniques Centre, Brunel University, Uxbridge, Middlesex, UB8 3PH, UK

[d] Cell-Mineral Research Centre, University of Sheffield, Kroto Research Institute, Sheffield S3 7HQ, UK

Abstract: TiAlN/VN multilayer coatings exhibit excellent dry sliding wear resistance and low friction coefficient, reported to be associated with the formation of self-lubricating V_2O_5. To investigate this hypothesis, dry sliding ball-on-disc wear tests of TiAlN/VN coatings on flat stainless steel substrates were undertaken against Al_2O_3 at 25 ^{0}C, 300 ^{0}C and 635 ^{0}C in air. The coating exhibited increased wear rate with temperature. The friction coefficient was 0.53 at 25 ^{0}C, which increased to 1.03 at 300 ^{0}C and decreased to 0.46 at 635 ^{0}C. Detailed investigation of the worn surfaces was undertaken using site-specific transmission electron microscopy (TEM) via focused ion beam (FIB) microscopy, along with Fourier transform infrared (FTIR) and Raman spectroscopy. Microstructure and tribo-induced chemical reactions at these temperatures were correlated with the coating's wear and friction behaviour. The friction behaviour at room temperature is attributed to the presence of a thin hydrated tribofilm and the presence of V_2O_5 at high temperature.

1 Introduction

Titanium nitride (TiN) with the B1 NaCl structure has been widely used as a hard wear-protective coating since the 1980s. Subsequently, TiAlN coatings were developed that provide much improved high-temperature oxidation resistance, up to 750–900 ^{0}C, and have consequently been used extensively for high-temperature cutting operations with minimum use of lubricant or dry machining [1]. Both the friction and wear performance of TiAlN can be improved through the quaternary addition of V, as monolithic Ti–Al–V–N coatings or as TiAlN/VN multilayers. TiAlN/VN multilayer coatings have alternating nanoscale dimensions of TiAlN and VN layers (typical period 3– 5 nm). They have exhibited superior hardness and sliding wear resistance (wear rate 1.26×10^{-17} $m^3N^{-1}m^{-1}$) with a lower friction coefficient (μ = 0.5 ± 0.1, Al_2O^3 ball counterpart, sliding speed 0.1 ms^{-1} and 5 N load) after ball-on-disc test at room temperature in comparison to other wear resistant coatings [2], e.g. TiAlN, TiAlN/CrN (specific wear rate 2.38×10^{-16} $m^3N^{-1}m^{-1}$, μ = 0.7–0.9 under similar test conditions). Laboratory dry sliding wear tests of TiAlN/VN coatings under ambient conditions (μ = 0.54, Al_2O_3 ball counterpart, sliding speed 0.1 ms^{-1} and 5 N load) yielded wear debris containing V_2O_5 detected by Raman spectroscopy [3]. The V_2O_5 has a melting point 674 ^{0}C [4] and inherently low friction, leading to suggestions that formation of this oxide is the key to low frictional behaviour of these coatings. High-temperature wear tests of TiAlN/VN multilayer coatings (V∼50 at.%) against Al_2O_3 showed increase of friction coefficient from 0.55 at 25 ^{0}C to 0.96 at 500 ^{0}C, followed by a sharp decrease to 0.18 at 700 ^{0}C [5]. Similarly, wear tests of Ti–Al–V–N monolithic films (2.40 at.% ≤ V ≤ 11.10 at.%) against an Al_2O_3 ball exhibited friction coefficients in the range of 0.6–0.85 at 25 ^{0}C, which increased to 1.1 at 500 ^{0}C and dropped to the range of 0.8–0.2 at 700 ^{0}C (friction coefficient value depended on the concentration of V) [6]. Wear studies of VN coatings by Gassner et al. [7] and Fateh et al. [8] confirmed the reduced friction coefficient associated with the formation of lubricious vanadium oxides, i.e. Magne´li phases at elevated temperatures. In particular, Fateh et al. compared the behaviour of TiN and VN under identical conditions. The TiN exhibited a high friction coefficient (0.5–0.7) at all temperatures, while the VN exhibited a decrease in friction with temperatures higher than 400 ^{0}C, showing a value as low as 0.25 at 700 ^{0}C. Using XRD and Raman spectroscopy, they observed a range of vanadium-based oxides on the worn surface of the VN, namely V_2O_5, VO_2 and V_6O_{13}. These agree well with static oxidation of VN [9] and TiAlN/VN [10] which suggested that oxidation started at 400 ^{0}C and 550 ^{0}C respectively and V_2O_5 was dominant on TiAlN/ VN higher than 638 ^{0}C.

The friction behaviour is dependent on the exact composition of the coating, not just the presence of V, as shown by the differences in behaviour of VN and TiAlVN, for example. The friction coefficient observed for TiAlN/VN (V∼50 at.%) and Ti–Al–V–N (2.40 at.% ≤ V ≤ 11.10 at.%) exhibited large differences, as described above, suggesting that the presence of Al and/or Ti increases friction at 500 ^{0}C. Increasing V from 2 at.% to 10 at.% in Ti–Al–N led to a decrease in friction from 0.85 to 0.73 at room temperature and 1.10–0.80 at 500 ^{0}C [6]. Further increasing V up to 50 at.% in TiAlN/VN showed a friction coefficient between 0.40 and 0.55 at room temperature, and 0.95 at 500 ^{0}C [5]. The effect is particularly marked at 700 ^{0}C when molten V_2O_5 is produced (μ = 0.8 with 2 at.%, μ = 0.25 with 25 at.%, and μ = 0.18 with 50 at.%).

The role of surface films as a direct result of frictional contact (so-called tribofilms [11]) remains a topic of some debate, largely because the structure of such films is not fully understood, but is known to vary from film to film. The tribofilm is most likely a compositional mixture of the two base materials and oxidation products caused by friction heating. A thin tribofilm is believed to be associated with low wear rates (so-called mild wear) and is believed to be a controlling factor in the observed friction coefficient. Equally, the observation of roll-like wear debris on worn surfaces is now relatively common and is believed to be associated with systems operating at low temperature that exhibit low wear rates. However, the structure of such roll-like wear debris has not been well studied and therefore the origin remains unknown.

The current work presents a detailed examination of the worn surface structure in order to understand the role of V in the coating in promoting low friction at high temperatures and the origin of high friction at lower temperatures. The same TiAlN/VN multilayer coating (V 55.2 at.%, Ti 28.5 at.% and Al 16.3 at.%) was used in our published oxidation study [10]. Focused ion beam (FIB) microscopy was used to produce site-specific transmission electron microscopy (TEM) cross-sections to study the structure of the worn surface at the region containing roll-like wear debris. Extensive energy loss spectroscopy (EELS) and electron diffraction was used to determine the local structure and bonding state in the surface tribofilm as a function of temperature. Fourier transform infrared (FTIR) and Raman spectroscopy was further used to investigate the structure of these surface layers. These techniques were used to address the following specific questions: (1) Can the surface tribofilms explain the friction behaviour as a function of temperature for multilayer TiAlN/VN? and (2) What is the true structure of the tribofilm and therefore how are V, Al, Ti and O involved in its formation?

2. Experimental procedures

2.1. Coating

TiAlN/VN multilayer coatings were deposited using the combined steered cathodic arc/unbalanced magnetron (UBM) sputtering (ABS™: arc-bond sputtering) technique using an industrial Hauzer HTC 1000-4 PVD coater. Deposition was undertaken in an Ar + N_2 atmosphere, with two TiAl targets (50:50 at.%, purity 99.99%) and two V (purity 99.8%) targets, and stainless steel substrates (AISI304). The coating process comprised three steps: (i) V^+ etching of the substrates in cathodic arc mode by applying a substrate bias of -1200 V to clean the surface and introduce ion-implantation for better adhesion; (ii) VN base layer deposition using UBM sputtering of V targets to introduce a stress gradient layer which further enhances the adhesion of the multilayer TiAlN/VN; (iii) TiAlN/VN multilayer deposition using UBM sputtering in Ar+N_2. A bias voltage of -75 V was applied on the substrates at a temperature of 450 ^{0}C during deposition. Full details of the deposition process are given elsewhere [2]. The coatings deposited on flat stainless steel disc substrates (AISI 304) were used for ball-on-disc wear tests. All the substrates had the same preparation procedure and were polished to a surface roughness R_a 0.020 μm before coating.

2.2. Wear testing

Dry sliding wear tests against an Al2O3 ball were undertaken in ambient air at room temperature (25 ^{0}C), 300 ^{0}C and 635 ^{0}C, respectively on a ball-on-disc tribometer (CSM high-temperature tribometer, Switzerland). An Al_2O_3 ball was utilized as the counterface due to its relative inertness, as it would not be expected to react with the coating, and because alumina has been widely utilized in wear testing of coatings, and therefore the current results can better be compared to those in the literature. The wear test conditions were: 1 N load, 0.05 m s^{-1} speed, radius of wear track 9 mm and various sliding distances for the different temperatures. Low sliding speed and load were used to minimize the friction heating. Humidity was recorded during wear sliding inside the enclosure chamber which houses the wear couple. The sliding distance was chosen to ensure that steady state wear was obtained (as shown by experiments that recorded wear as a function of distance), but without so much wear that the thinning of the coating resulted in a change in the effect of the substrate. For the tests at elevated temperatures, the specimens were heated to the required temperature prior to the start of sliding on the coating surfaces. A ramping rate of 20 ^{0}C min^{-1} was used to ensure the TiAlN/VN starting surface exhibited its equilibrium structure, i.e. for the test at 635 ^{0}C the starting surface would have been predominantly V_2O_5 on the basis of a prior static oxidation study [10].

2.3. Surface and cross-section characterization

Wear track depth, width and surface roughness were examined using a surface profilometer (Taylor-Hobson Talysurf 120L, UK) with a 2 μm radius diamond stylus and surface height resolution 5 nm. The wear surfaces were initially characterized by scanning electron microscopy (SEM, JEOL 6400, Japan). Cross-sections of the worn surfaces were prepared for TEM using a FIB (FEI Quanta 200, Holland). A carbon coating was deposited prior to FIB milling to protect the worn surface layer upon exposure to the Ga^+ beam. Subsequently, a Pt layer was deposited on top of the area of interest before Ga^+ milling. TEM (JEOL 2010F, Japan) in conjunction with energy dispersive X-ray spectroscopy (EDX, Oxford Instruments Link Isis, UK) and electron energy loss spectroscopy (EELS, Gatan GIF2000, USA) were employed to analyse the worn surface. Composition data on the worn surface was obtained in EDX mode on the 2010F field emission gun (FEG) TEM with a nominally 1.0 nm electron probe. EELS measurements were made in conventional TEM diffraction mode (image coupling to the spectrometer). Sample areas were chosen that were thin enough to avoid the need for spectral deconvolution. For each area C K, N K, Ti $L_{2,3}$, V $L_{2,3}$ and O K-edges and associated low loss spectra were collected. The 0.6 mm EELS entrance aperture was used, giving a collection semi-angle β of 4.0 mrad at a camera length of 8 cm. The energy resolution was 1.2 ± 0.1 eV for all the EELS measurements.

FTIR and Raman spectroscopy were performed on the plan-view worn surfaces, including regions where wear debris had accumulated to further characterize structural changes. A micro-FTIR spectrometer (PerkinElmer Spotlight FTIR imaging system) was used to examine the worn surfaces after tests at 25 ^{0}C and 300 ^{0}C. This instrument can record both the IR image and spectrum at each scanning point. The spectra and images were acquired in reflectance mode, spot size 6.25 μm, spectral resolution 4 cm^{-1}, wave number from 650 cm^{-1} to 4000 cm^{-1}. A

Renishaw inVia Raman spectrometer (Renishaw plc, UK) was employed to conduct point analysis on the worn surfaces with a 20 mW Ar laser (λ = 514.5 nm) and a 50x objective lens after wear tests (spot size of 2 μm).

Table 1 Wear and friction data from the ball-on-disc wear tests of TiAlN/VN coatings at various temperatures.

	25 ^{0}C	**300 ^{0}C**	**635 ^{0}C**
Mean friction coefficient, μ	0.53 ± 0.02	1.03 ± 0.06	0.46 ± 0.02
Laps run/sliding distance (m)	20,000/1129.4	10,000/565.5	2500/141.3
Time duration test at the temperature (min)	378	188	50
Wear scar surface roughness Ra (μm)	0.067	0.060	0.670
Mean width of wear track (μm)	119 ± 5	100 ± 5	101 ± 5
Specific wear rate; K (m^3 N-1 m-1)	2.3 x 10-15	5.0 x 10-15	90.0 x 10-15
Humidity	22%	5%	–

Test conditions: 6 mm Al_2O_3 ball counterpart, linear sliding speed 0.05 m s-1, 1 N load, wear track radius 9 mm. Humidity was recorded during wear sliding inside enclosure chamber.

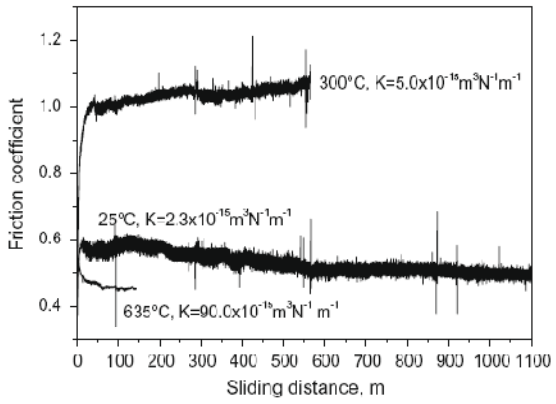

Fig. 1. Friction coefficient curves of TiAlN/VN coatings as a function of sliding distance tested at 25 ^{0}C, 300 ^{0}C and 635 ^{0}C (test conditions: 6 mm Al_2O_3 ball counterpart, sliding speed 0.05 m s-1, 1 N load, track radius 9 mm).

3. Results

3.1. Specific wear rates and friction coefficient of TiAlN/VN

Table 1 lists the test parameters, friction and wear results. Fig. 1 shows the friction curves as a function of sliding distance. Steady state wear was obtained after a short sliding distance of <50 m for all temperatures, with the average friction coefficients then being 0.53 at 25 ^{0}C, sharply increasing to 1.03 at 300 ^{0}C and dropping to 0.46 at 635 ^{0}C. The specific wear rate (K) of the coating was low at 25 -C (2.3 x 10-15 m^3 N-1 m-1) and doubled at 300 ^{0}C. A sharp increase in wear rate was observed at 635 ^{0}C with a value of 90.0 x 10-15 m^3 N-1 m-1. The roughnesses of the worn surfaces at 25 ^{0}C and 300 ^{0}C, measured in the smoother regions, were similar despite the factor of two difference in friction coefficient. Roughness of the worn surface after the test at 635 ^{0}C was 0.67 μm, an order of magnitude higher than at room temperature.

3.2. Plan view studies of the worn surface microstructure at 25 ^{0}C, 300 ^{0}C and 635 ^{0}C

3.2.1. General worn surface structure

Fig. 2 shows typical scanning electron microscopy (SEM) plan-view images of the worn surfaces at the three temperatures. The wear track surface at 25 ^{0}C (Fig. 2a and b) was smooth,

119 ± 5 lm wide, with wear debris piled up on either side (with the bright contrast). On top of the wear track surface roll-like debris were present, with the long axis of the roll perpendicular to the sliding direction (Fig. 2b). The rolls were 0.5–3 μm long, 20–200 nm in diameter. Similar rolls have been widely reported for the mild wear of hard materials, e.g. in the sliding wear of SiC–Al_2O_3 nanocomposites [12], Si_3N_4 [13], Al_2O_3 [14] and diamond-like carbon films [15]. The structure and origin are still a matter of debate. Longitudinal TEM cross-sections along the sliding direction were extracted using FIB, for example, at the location indicated by the white arrow bar (Fig. 2b) to investigate the outermost worn surface, including the roll-like wear debris (Section 3.3.1). The low wear rate and the presence of the roll-like debris indicate mild adhesive wear at 25 ^{0}C.

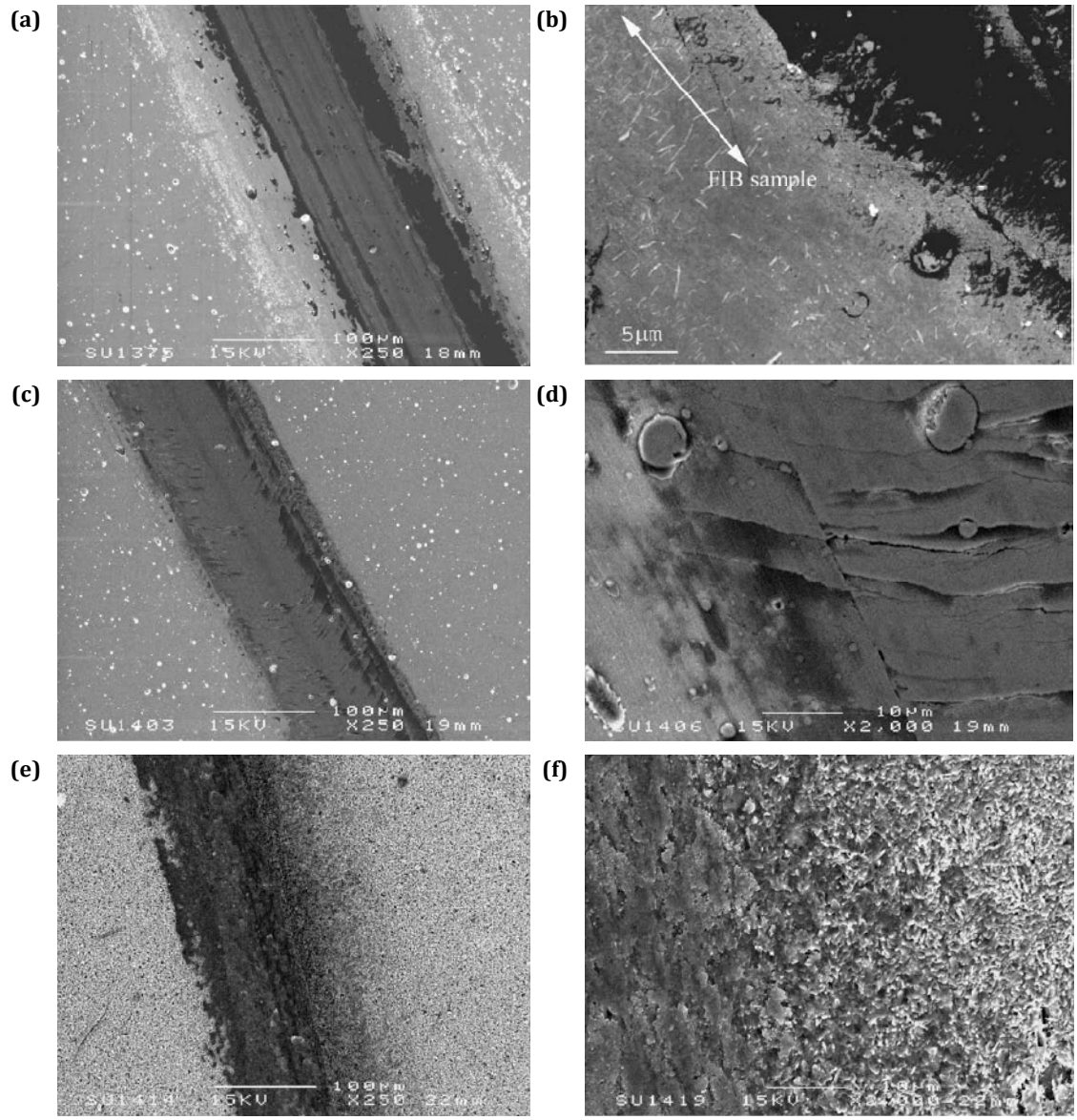

Fig. 2. SEM micrographs of the worn surfaces after ball-on-disc tests at 25 ^{0}C (a and b), 300 ^{0}C (c and d) and 635 ^{0}C (e and f).

Fig. 2c and d shows the worn surface after the test at 300 ^{0}C. In contrast to the 25 ^{0}C wear track, loose wear debris were absent at either side of the track. Closer inspection of the worn surface confirmed that there were no roll-like wear debris on the track, but a number of half-

moonshaped cracks. Such half-moon-shaped cracks are typically found in sliding contact conditions of hard materials that experience large surface tractions (i.e. high coefficient of friction) [16]. The inclusion-like particles in Fig. 2d are the growth defects of the coating, a typical defect caused by arc discharge during V+ etching step during deposition [17]. The cracks were not all associated with the growth defects. Despite the high friction coefficient at 300 ^{0}C, the wear rate remained relatively low, and worn surface was as smooth as that tested at 25 ^{0}C apart from the cracks, indicating a similar wear mechanism at this temperature to the one at room temperature. Additional SEM examination confirmed that the coating that had not been subject to the sliding contact was unchanged after heating at 300 ^{0}C, consistent with our previous oxidation study.

Fig. 2e and f shows the worn surface of TiAlN/VN after testing at 635 ^{0}C. Outside the wear track, the coating surface was completely covered with oxide scale. Fig. 2f is a close inspection of the edge of the wear scar, showing the growth of the oxide (right-hand side) and the rough worn surface (left-hand side). The rough worn surface is consistent with high wear rate oxidational wear. It took 30 min to heat the specimen from 25 ^{0}C to 635 ^{0}C and 50 min to complete the sliding test. This would have resulted in the surface being covered in a thin oxide prior to the test. XRD of the surface confirmed that it consisted mainly of V_2O_5 and TiO_2 (rutile), consistent with the isothermal study of the coating [10].

3.2.2. FTIR of worn surfaces at 25 ^{0}C and 300 ^{0}C

The reflectance micro-FTIR study was undertaken to understand the extent of hydration of the surface tribofilm, the structure of which is discussed later in Section 3.3. Fig. 3 shows the results of the worn surface of TiAlN/VN against Al2O3 tested at 25 ^{0}C. Fig. 3a is an optical image giving an overview of the wear track. Fig. 3b shows spectra from the as-deposited coating (labeled 1), the central wear track where rolls were frequently observed (labeled 2) and loose wear debris outside at the edge of the track (labeled 3). The central wear track had an almost identical spectrum to the unworn as-deposited surface (compare 2 with 1). The spectrum from the loose wear debris at the edge of the track showed a –OH stretching band at ~3300 cm^{-1} and a –OH bending band at 1635 cm^{-1} (arrows), which are significantly stronger than the central wear track (compare 3 with 2). The loose wear debris were composed of a large population of fine particles accumulated at either side of the track. These wear debris particles aggregated to several microns in size, significantly larger than the roll-like debris adhered to the worn surface, so that the signal from wear debris aggregates would have inevitably been larger than from either the tribofilm or the roll-like wear debris. Although the spectrum from the loose wear debris has a broad peak centred at 3300 cm^{-1}, suggesting the presence of an –OH bond, this peak may be due to the presence of water, as indicated by the peaks at 1635 cm^{-1}. In order to exclude free water moisture trapped inside the wear debris aggregates, the wear track was heated in air at 110 ^{0}C for 1 h to vaporize water moisture and was then immediately re-examined, as shown in Fig. 3b (labelled 4). The –OH in free water is believed to be associated with the peaks at 1635 cm^{-1}and 3300 cm^{-1}, whereas –OH in hydroxyl mainly appears at 3300 cm^{-1}. It is evident that the heated debris still showed the –OH stretching band at 3300 cm^{-1}, whereas the –OH bending signal at 1635 cm^{-1}appeared with much less intensity. This could indicate the presence of hydroxides in the wear debris. Fig. 3c is a false-colour1 image of the

worn surface using micro-FTIR spectroscopy, showing the location of molecules with absorption band intrinsic of stretching –OH (3300 cm-1). It highlights the distribution of –OH-rich regions, which are mainly the loose wear debris aggregates at the side of the track.

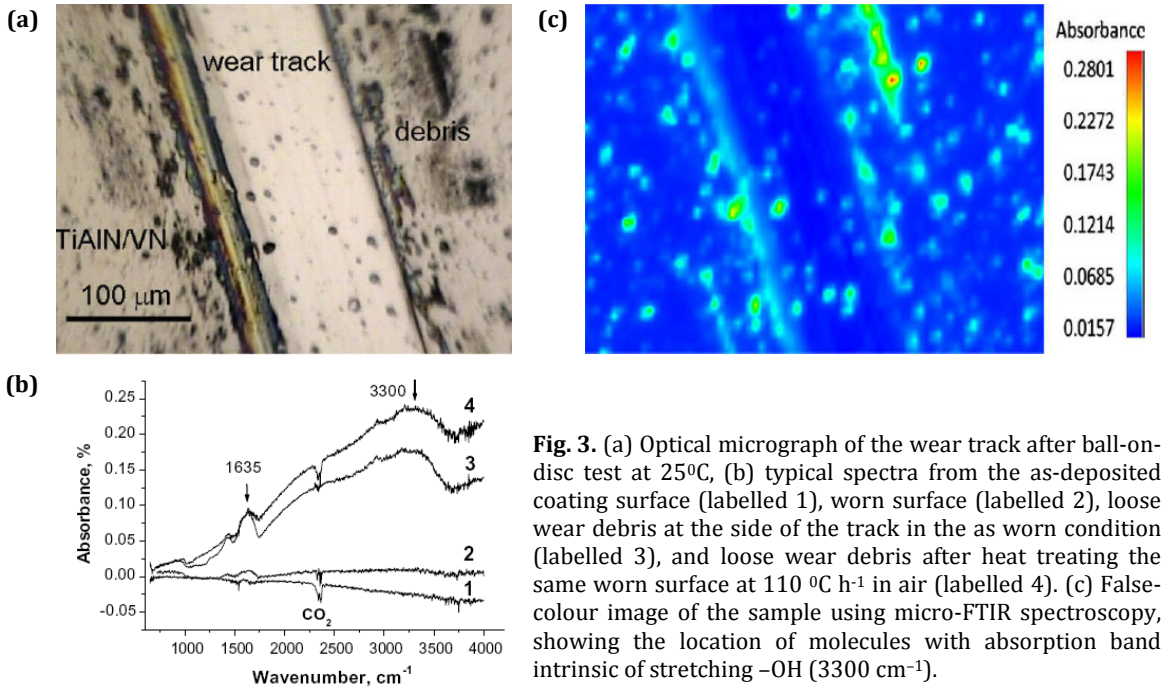

Fig. 3. (a) Optical micrograph of the wear track after ball-on-disc test at 25^{0}C, (b) typical spectra from the as-deposited coating surface (labelled 1), worn surface (labelled 2), loose wear debris at the side of the track in the as worn condition (labelled 3), and loose wear debris after heat treating the same worn surface at 110 ^{0}C h^{-1} in air (labelled 4). (c) False-colour image of the sample using micro-FTIR spectroscopy, showing the location of molecules with absorption band intrinsic of stretching –OH (3300 cm^{-1}).

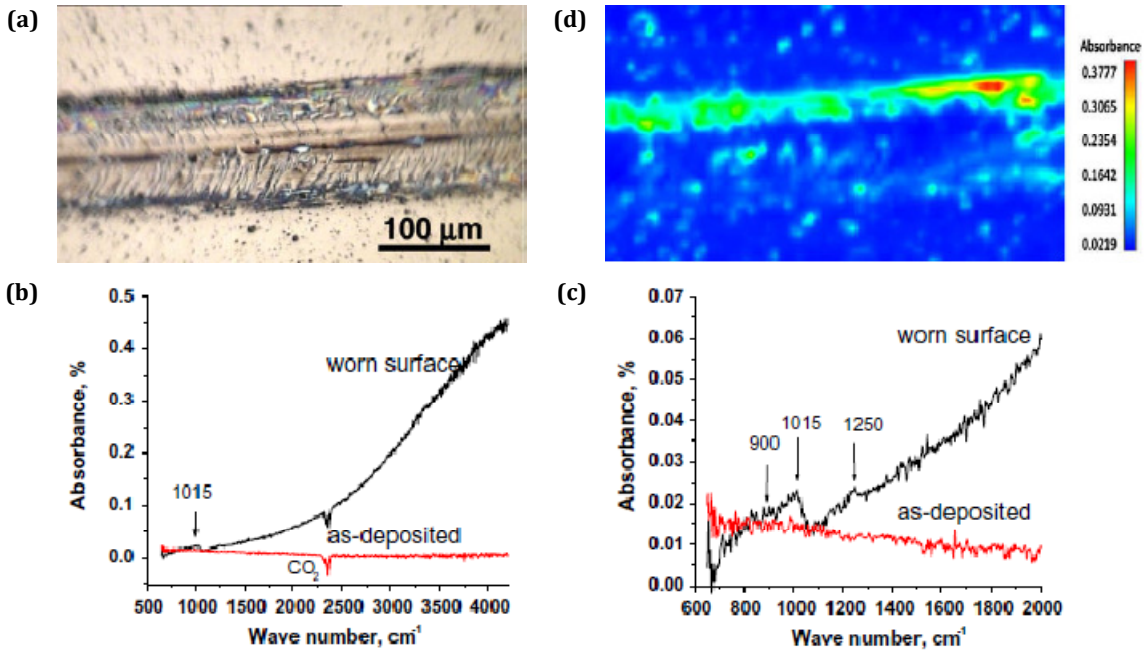

Fig. 4. (a) Optical micrograph of the wear track after ball-on-disc wear at 300 ^{0}C and (b) IR spectra from the as-deposited coating and worn surfaces with –OH bands absent. (c) Enlarged portion of spectra in (b) shows a peak at 1015 cm^{-1}, suggesting V=O bonding. (d) False-colour image of the sample using micro-FTIR spectroscopy, showing the location of molecules with absorption band intrinsic of V=O (1015 cm^{-1}).

FTIR was also undertaken on the worn surface of the TiAlN/VN against Al2O3 at 300 ^{0}C. Fig. 4a is an optical image of the track. Fig. 4b shows typical spectra from the as-deposited surface and a region at the edge of the worn surface. The –OH bands at 1635 cm-1and 3300 cm-1are all

absent. An enlarged portion of the spectra (Fig. 4c) in the range between 2000 cm-1and 650 cm-1 shows bands at ~900 cm-1 and ~1015 cm-1, which are in line with bridging bands of V–O–V (~900–940 cm-1) and V=O (1030 cm-1) [18]. Fig. 4d is the micro-FTIR image formed using the 1015 cm-1 band, which has high intensity on the worn surface, in particular the top edge (the inner circle to the sliding rotation centre).

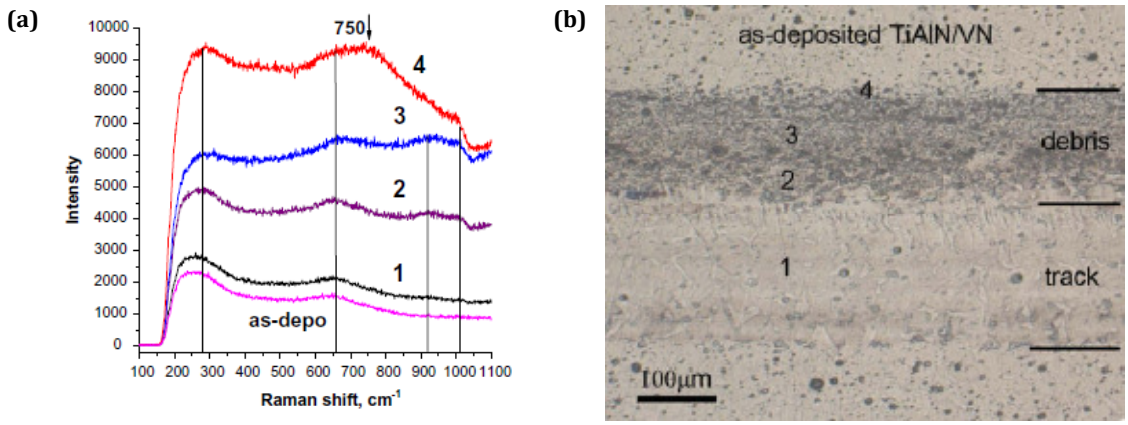

Fig. 5. (a) Raman spectra of typical locations on the worn surface after testing at 25^{0}C, as labeled in (b), an optical micrograph of the worn surface, 1 denotes typical flat featureless area on the worn surface, 2 and 3 are at the edge of wear track with ~50 μm interval, 3 is wear debris further away from the edge.

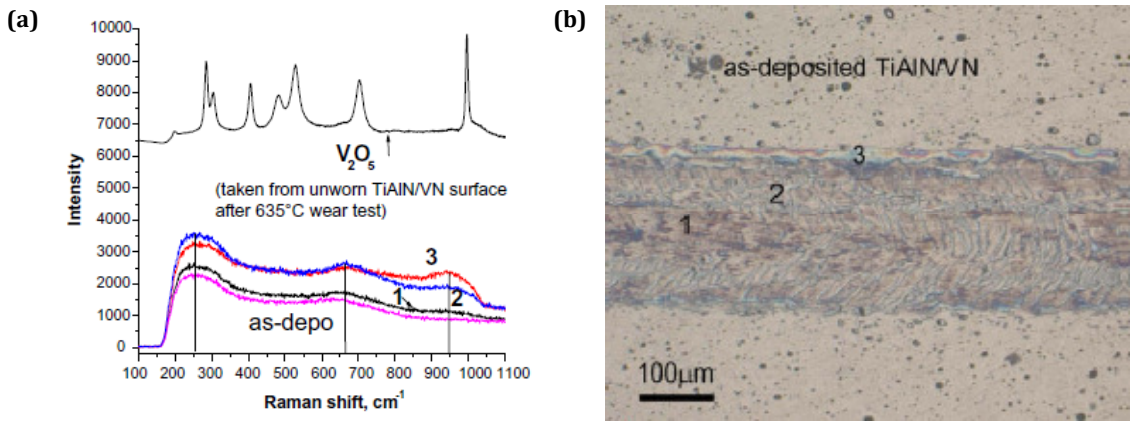

Fig. 6. (a) Raman spectra of typical locations on the worn surface after testing at 300 ^{0}C, as labelled in (b), an optical micrograph of the worn surface, 1 denotes the central flat area, 2 is the shaded area between cracks, 3 is at the edge of the wear track. An additional spectrum in (a) was taken from unworn oxidized surface of TiAlN/VN after 635 ^{0}C test and identified as V_2O_5.

3.2.3. Micro Raman study of the worn surface after test at 25 ^{0}C and 300 ^{0}C

Raman microscopy was used to probe local changes in chemical structure from the wear track centre towards loose wear debris at the outside of the track. Fig. 5 shows the Raman spectra and an optical micrograph indicating the locations (1–4) on the wear track from the test at 25 ^{0}C. No chemical change was detected at the central smooth wear track (location 1) as compared with the as deposited coating (Fig. 5a). Raman bands at 920 cm-1 and 1015 cm-1 appeared for the spectra taken from the wear debris (locations 2 and 3) at the edge of the wear track. These Raman bands are complementary to the IR absorbance peak at ~900 cm-1 and 1015 cm-1, which may be assigned to V–O–V and V=O bonding, a sign of oxidation of VN. As the probe further moved outside the wear track (location 4), debris particles were larger, an unknown

band at 750 cm-1 was observed. Fig. 6 shows Raman spectra (a) and an optical micrograph (b) indicating the locations on the wear track where the spectra were collected for the test at 300 ^{0}C. The worn surface exhibited cracks mainly located from the edge to 1/3 of the width of track. The central 1/3 of the track contained fewer cracks, and exhibited a different interference colour (brown) compared to the remainder of the track (blue/orange). Again there was minimal change in the Raman spectra from the smooth region (location 1) of the worn surface compared to the as-deposited surface. Raman spectra between the cracks (location 2) and at the edge (location 3) of the wear track showed a V–O–V bridging band at 940 cm-1, indicating oxygen containing wear debris layer on the surface and trapped in the cracks. There was no significant difference between the Raman spectra from the tribofilms at different locations on the worn surface. Fig. 6a shows an additional Raman spectrum taken from unworn/oxidized surface after the coating was tested at 635 ^{0}C. The spectrum has strong bands at 286 cm-1, 405 cm-1, 701 cm-1, and 995 cm-1. The number, position and shape the bands are identical to a V_2O_5 standard presented by Constable et al. [3]. On the basis of our previous oxidation study [10], V_2O_5 was the dominant phase on the surface after 30 min at 635 ^{0}C. Therefore, we take this spectrum as typical of V_2O_5. Comparing all the Raman spectra, no evidence of V_2O_5 was found at the worn surfaces at 25 ^{0}C and 300 ^{0}C.

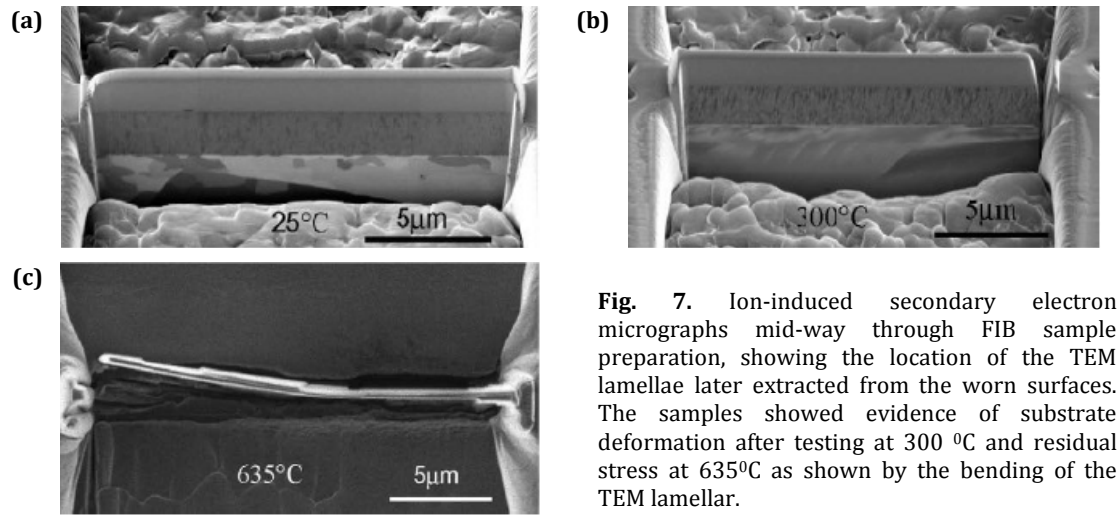

Fig. 7. Ion-induced secondary electron micrographs mid-way through FIB sample preparation, showing the location of the TEM lamellae later extracted from the worn surfaces. The samples showed evidence of substrate deformation after testing at 300 ^{0}C and residual stress at 635^{0}C as shown by the bending of the TEM lamellar.

3.3. Cross-sectional studies of the worn surfaces

FIB was used to extract cross-sectional TEM thin foils from typical features on the worn surfaces from the region indicated in Fig. 2b. Fig. 7 shows ion-induced secondary electron images mid-way through sample preparation. Note the equiaxed stainless steel substrate after wear at 25 ^{0}C in contrast with the plastic deformation bands towards the sliding direction after wear at 300 ^{0}C. In addition, the samples showed evidence of residual stress after testing at 300 ^{0}C and 635 ^{0}C as shown by the bending of the TEM lamellar as they were cut from the substrate. This was particularly marked for the sample at the higher temperature.

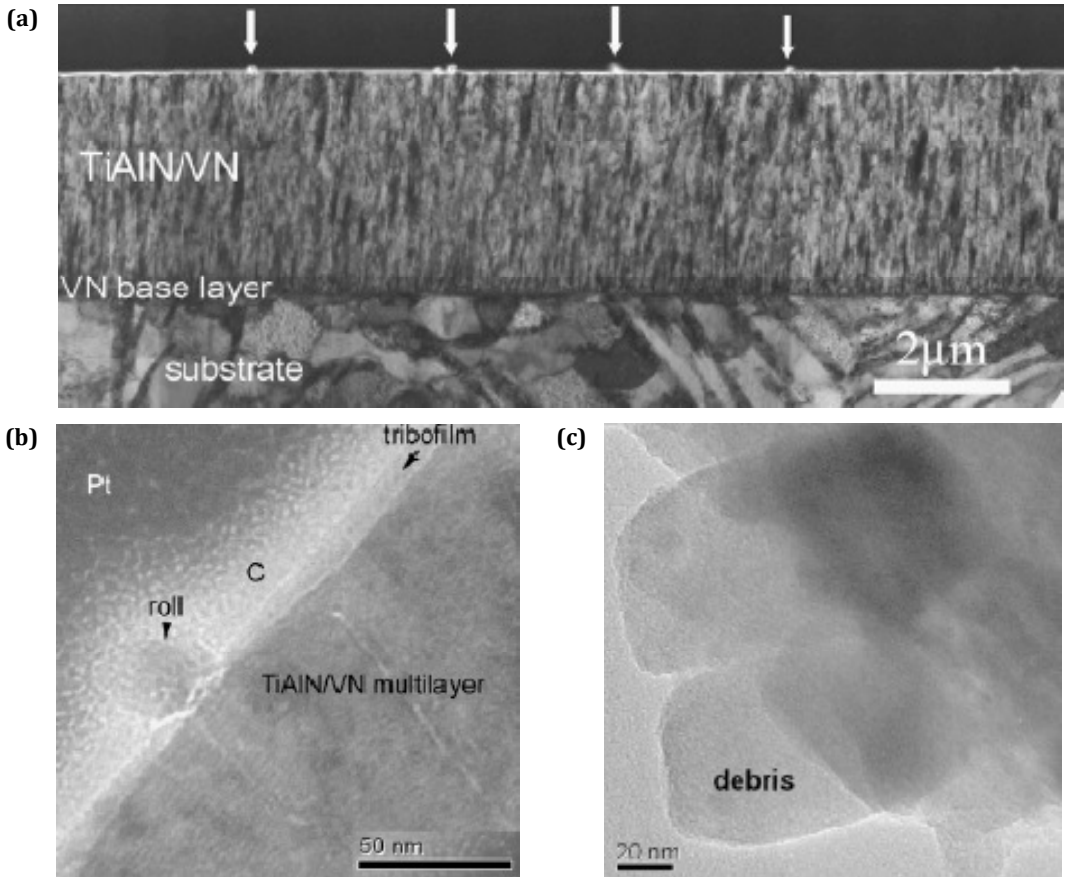

Fig. 8. Bright-field TEM images from cross-sections of the worn surface after testing at 25 ^{0}C. (a) TiAlN/VN on top of the stainless steel substrate. There was no evidence of plastic deformation in the coating or substrate. Surface tribofilm and the roll-like wear debris are shown on the top of the coating (arrows). (b) Detail of the tribofilm and a roll. (c) Amorphous loose wear particles on holey carbon film.

3.3.1. Test at 25 ^{0}C

Fig. 8 gives bright-field TEM micrographs of cross-sections of worn surfaces at 25 ^{0}C. The structure of the coating, as shown in Fig. 8a, comprises (from the bottom to the top) equiaxed grain steel substrate, the VN base layer and the TiAlN/VN coating, with the columnar growth easily seen. At the very top of the coating a thin layer tribofilm is present. In addition, the roll-like wear debris particles, of diameter 5–40 nm, are just visible in Fig. 8a (arrowed). Closer inspection of the columnar grain structure of the coating and the substrate showed no evidence of cracks, and no sign of plastic deformation. Fig. 8b highlights a roll and the tribofilm on the worn surface. It comprises the multilayer coating, thin surface tribofilm, carbon and platinum deposition. Note that the multilayer structure of the coating was preserved right up to the tribofilm. The tribofilm is amorphous with a thickness that varied along the length of the worn surface in the range 2–20 nm. The roll-like wear debris was also amorphous, attached to the surface tribofilm by a thin amorphous layer. Loose wear debris were lifted from the side of the wear track and deposited on a thin carbon film for TEM examination (Fig. 8c). The wear debris comprised irregular-shaped particles between 0.05 μm and 5 μm. Most of the particles collected by the holey carbon TEM grid were electrontransparent and amorphous.

Table 2 Composition (at.%) of tribofilms and adjacent coatings tested at 25 ^{0}C and 300 ^{0}C from standardless EDX analysis, error ± 0.5%.

		Al	Ti	V
Loose wear debris	25 ^{0}C	33	21	46
Rolls		26	22	52
Tribofilm		29	22	49
Coating		28	21	51
Tribofilm	300 ^{0}C	31	23	46
Coating		23	21	46

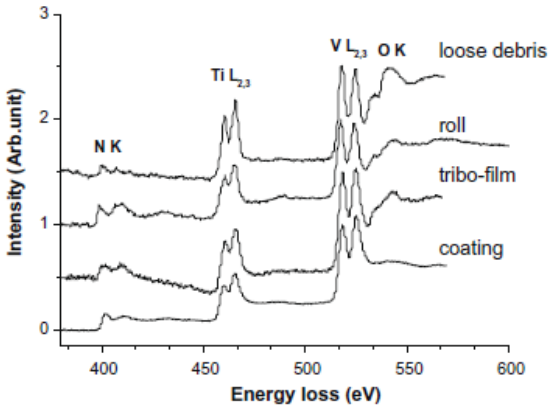

Fig. 9. Normalized experimental EEL spectra from coating, tribofilm, rolls, and loose wear particles after testing at 25 ^{0}C.

Table 2 gives the composition determined by EDX point analysis of the typical positions at the worn surface TEM cross-sections tested at 25 ^{0}C. A similar concentration of Al, Ti and V was observed for all the debris compared to the bulk. EELS was employed to analyse the O and N in these areas. The samples prepared by FIB generally had a thickness $t > 0.5\lambda$ (where λ is mean free electron path), making EELS analysis unreliable because of plural scattering. However, the worn surface region itself was slightly thinner, around $t \approx 0.5\lambda$, thereby allowing acceptable EELS analysis. Fig. 9 compares normalized and background subtracted EEL spectra from all the features shown in Fig. 8, namely the coating, tribofilm, the roll-like wear debris and the loose wear debris. The spectrum from the coating was consistent with that published elsewhere (e.g. see Ref. [19]). For all of the tribofilm, the roll-like wear debris and the loose wear debris, N K, Ti $L_{2,3}$, V $L_{2,3}$ and O K-edges are all present, suggesting a form of $(TiAlV)N_xO_y$ (Al is not included in a spectrum here as the Al K is at 1560 eV, but was present as determined by EDX). The N intensity was lower in the loose wear debris compared to the tribofilm and roll-like debris, while the O was higher and the Ti was approximately constant. The V L_2/L_3 ratio changed from the coating to the tribofilm and the wear debris. This was associated with the increased O K, indicating that progressive oxidation of V begins at the tribofilm of the worn surface. In conjunction with this change in the shape of the V $L_{2,3}$ there is also a pronounced change in the shape of the N K edge, with the second peak at ~410 eV becoming increasingly dominant as the V L_3 increased and the L_2 decreased. This is consistent with a variation in the degree of sub-stoichiometry, which is common in VN_x compounds [20].

3.3.2. Test at 300 ^{0}C

Fig. 10a and b shows bright-field TEM micrographs of cross-sections of the worn surface at 300 ^{0}C. The section again comprises the steel substrate, base layer (VN) and columnar TiAlN/VN

coating. In contrast to the structure at 25 ^{0}C, the stainless steel substrate and the TiAlN/VN columnar grains had undergone plastic deformation. Extensive plastic deformation had occurred in the substrate. In addition, the TiAlN/VN columnar grains were tilted ~12^0 towards the sliding direction, which had resulted in cracking along the columnar grain boundaries, with more cracks situated at the lower half of the TiAlN/ VN, as indicated by the arrows in Fig. 10b. A number of cracks ran through the columnar grain boundaries, extending 50–100 nm below the interface into the steel substrate, suggesting that adhesion at the interface between the coating and substrate was excellent. In addition, some small cracks were present in the steel substrate just below the base layer, running parallel to the coating surface. No evidence of delamination between the baselayer and the steel substrate was observed. Fig. 10c shows a fractured step which arose from a crack through the columnar grain boundary. A tribofilm was observed across the entire outer surface, which provided a remarkably flat surface, even where it passed over a crack. Fig. 10d gives a detailed view of the outer worn surface region. The multilayer structure of the coating was preserved up to the tribofilm. The tribofilm itself was amorphous, but appeared to contain two layers that gave slightly different contrast in the bright-field TEM image. Such contrast changes were not observed in the 25 ^{0}C worn surface. EDX analysis of the tribofilm and the coating was included in Table 2.

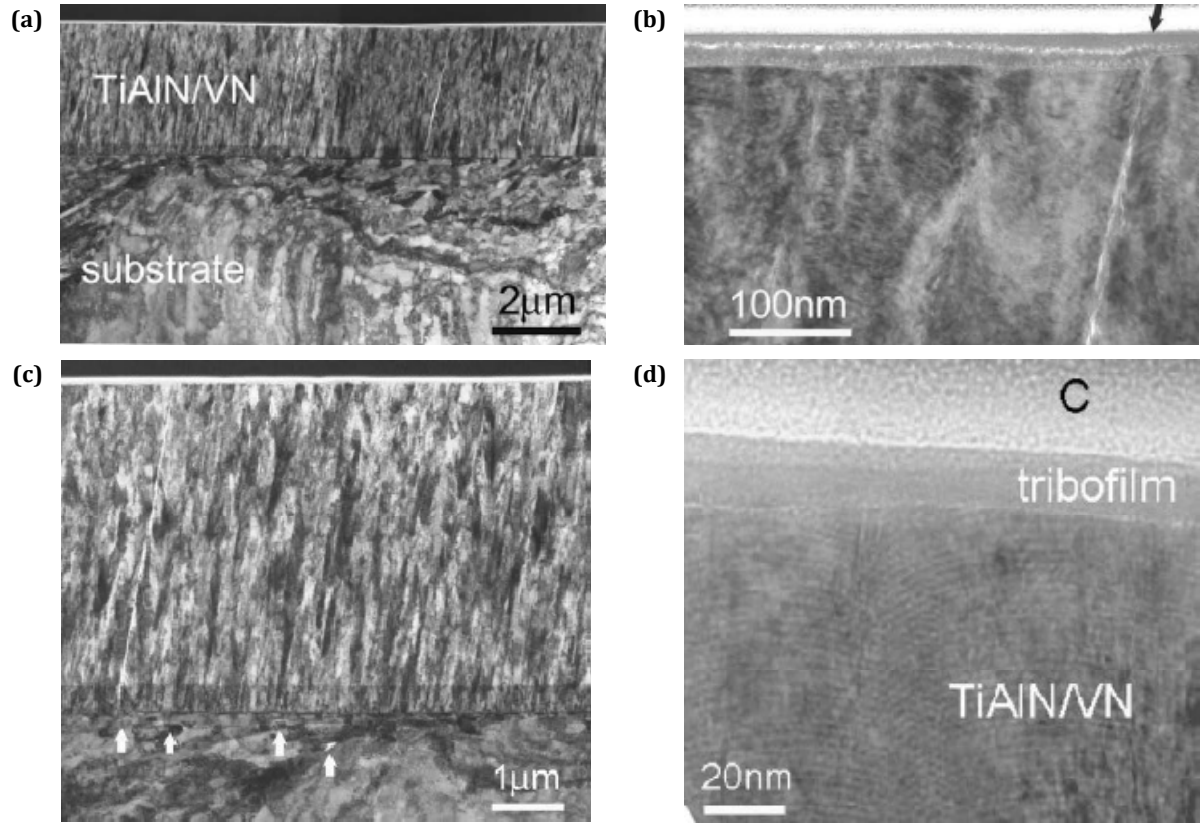

Fig. 10. TEM bright-field images of cross-sections of the worn surface tested at 300^{0}C. (a) General image showing substantial deformation in the substrate to a depth of ~5 μm, and bending of the columnar structure in the coating in the direction of sliding. (b) Detail showing cracks running along the columnar grain boundaries down to the substrate, and smaller cracks in the substrate itself. (c) A crack in the coating that produced a step on the coating surface. Note the continuous tribofilm above the crack. (d) Detail of the tribofilm on top of the coating, which exhibited two layers of differing contrast, and the retention of the multilayer structure in the coating up to the interface with the tribofilm.

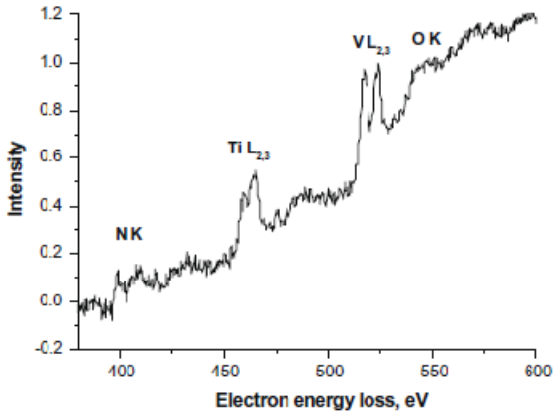

Fig. 11. EEL spectrum of the tribofilm formed after wear at 300 ^{0}C.

Fig. 11 shows a typical EEL spectrum of the tribofilm taken of the test at 300 ^{0}C, showing the presence of N, Ti, V and O, suggesting that oxidation occurred in the tribofilm. However, the TEM sample was too thick for a detailed study of the near edge fine structure of the core loss of ionization edges using EELS.

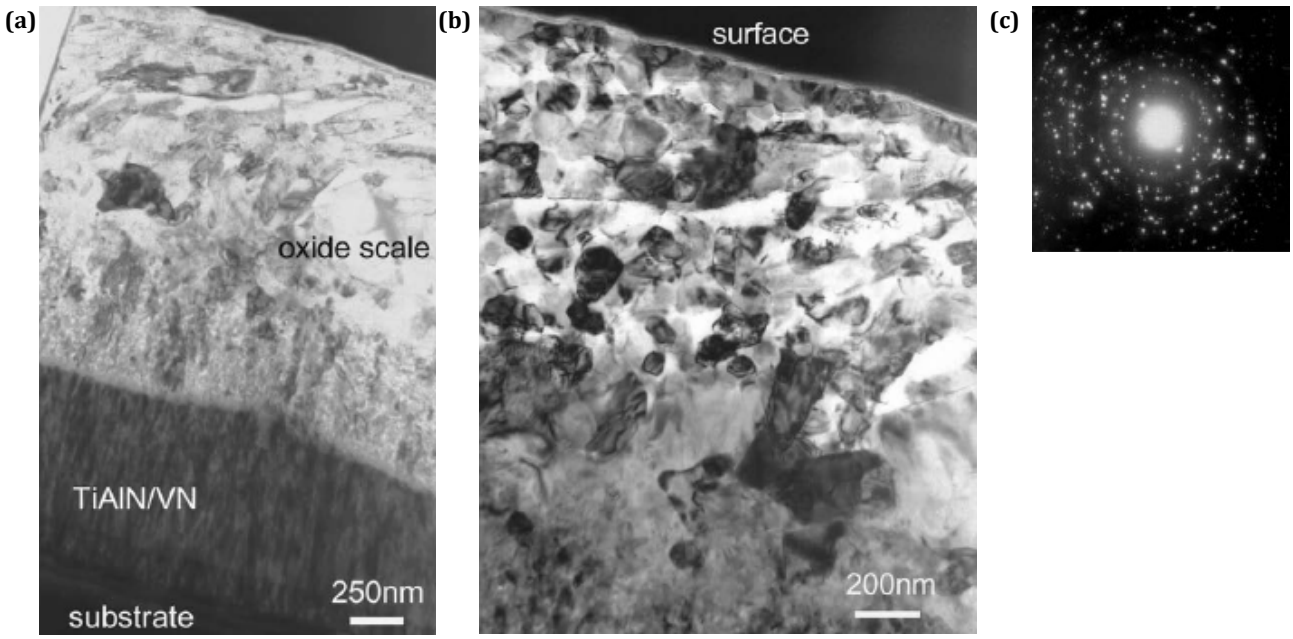

Fig. 12. Bright-field TEM micrographs of the worn surface tested at 635 ^{0}C (a and b), b is at a higher magnification than a, highlighting the contacting surface.) and a selected area diffraction pattern (c) confirmed the surface particles were mainly V_2O_5.

3.3.3. Test at 635 ^{0}C

The test at 635 ^{0}C exhibited a low friction coefficient of 0.46, in line with other observations for this coating, which the literature has suggested is a result of the formation of V_2O_5. Fig. 12a gives a TEM image of a FIB prepared sample, cut from the centre of the wear track in the longitudinal direction. Half of the original coating had been consumed at this temperature, and an oxide scale of almost double the residual coating thickness had been produced. However, the sliding contact resulted in attrition of the oxide particles to form a layer ~500 nm thick, in which fine, roughly equiaxed oxide particles had formed a relatively compact layer. Furthermore, a thin (~50 nm) outer layer can be seen which comprised a single layer of

equiaxed crystals, which provided the contacting surface (Fig. 12b). These were of a similar size to the crystallites in the region just below, but the region below was generally porous as a result of extensive volume expansion when nitrides were transformed to oxides [10]. Selected area diffraction (Fig. 12c) indicated evidence of mainly V_2O_5 with possibly VO_2. No evidence of surface-preferred orientation was found as a result of attrition, again suggesting that wear took place on top of the readily oxidized surface.

STEM/EDX was used to investigate the composition distribution of the surface scale (Fig. 13). It showed that the outer region of equiaxed crystals was dominated by V, with very little Al or Ti detected, consistent with the V_2O_5 phase identified by XRD and electron diffraction. This suggests that the surface layer was derived from the break-up of the large V_2O_5 crystals. Below the V_2O_5 layer TiO2 was interspersed by AlVO4 particles. This is consistent with static oxidation studies of TiAlN/VN at 638 ^{0}C [10].

Fig. 13. Cross-section of the worn surface tested at 635 ┐ C. STEM dark-field image shows the crystalline nature of the surface and the evidence of plastic deformation and corresponding EDX maps of Ti, Al and V from the same region.

4. Discussion

4.1. Friction behaviour at 25 ^{0}C and 300 ^{0}C

At both 25 ^{0}C and 300 ^{0}C, the outer worn surface was covered in a tribofilm. It is generally believed that the friction is strongly dependent on the presence and properties of a tribofilm, as the interfacial shear strength of the film will be a strong contributor to the resistance to motion. In many systems the formation of such tribofilms is engineered, for example through the use of additives to oil-based lubricants (e.g. zinc dialkyl-dithio-phosphate (ZDDP)). In the present work the marked difference in friction between room temperature and 300 ^{0}C must have been because of important differences in the properties of the tribofilm.

At both room temperature and 300 ^{0}C the tribofilm was amorphous. The film was somewhat thicker at 300 ^{0}C (by about 25 nm), but it would seem very unlikely that this would explain the difference in friction. In any event, it is likely that the thickness of such a film varies across the worn surface and therefore the difference was probably down to sampling statistics. The TEM (Figs. 8–11) together with EDX analysis (Table 2) indicated that, for both temperatures, the tribofilm had a similar composition to the coating, except that some nitrogen had been replaced by oxygen, indicating tribo-induced oxidation. The N content of the tribolayer was similar to that in the rolls, but was much less in the wear debris. The tribo-oxidation was also supported by evidence of V–O–V and V=O bonding in the worn surfaces at 25 ^{0}C and 300 ^{0}C detected by Raman spectroscopy. The FTIR indicated that the tribolayer was hydrated for the room temperature tests. The hydrolysis of AlN occurs by the thermodynamically favourable reaction [21,22]: $AlN + 2H_2O = AlOOH$ (amorphous) + NH_3.

The amorphous AlOOH can age further with water to give crystalline bayerite Al(OH)3. However, no crystallization of the tribolayer was observed, probably because the inadequate concentrations of the –OH ions and water [23]. As a result, amorphous monohydroxide remained at the surface. In contrast, at 300 ^{0}C, there was no evidence of –OH bands in the FTIR spectra. It is clear that the low-temperature hydrated tribofilm promoted relatively low friction, but as soon as the temperature was increased, the monohydrate was transformed to an amorphous (TiAlV)NxOy, which appears to have inherently higher friction.

It is interesting to note that at 300 ^{0}C, the worn surface comprised an amorphous layer. Fateh et al. [8] observed vanadium oxides, including V_2O_5, through Raman spectroscopy after testing of VN against Al2O3 at 400 ^{0}C on the surface using the same wear test equipment design as used in the current work. The V_2O_5 was found together with an increased friction coefficient compared to 25 ^{0}C, strongly suggesting that the V_2O_5 is not always necessarily associated with low friction. While the frictional heating is not known, the use of a sliding speed of 0.1 m s^{-1} suggests that it would have been minimal.

The fundamental difference in the properties of the film was shown by the presence of roll-like wear debris at room temperature, but not at 300 ^{0}C. The origin of the roll-like wear debris has been the subject of debate for some time. The observation that it had the same structure and composition as the tribolayer strongly suggests that it came from the tribolayer. The rolls are only observed at room temperature, strongly suggesting that hydration is important. The uniform structure of the rolls is an important observation, since it shows that the roll-like wear debris on the worn surface of TiAlN/VN did not form through delamination of the tribolayer, followed by the amorphous material being rolled up in a manner analogous to rolling up a carpet. The homogeneous structure suggests that the shape was formed through viscous flow to a round cross-section in order to minimize surface energy. Thus, this suggests that the rolls formed through the ploughing action of the counterface asperities displacing the surface tribofilm followed by a change in shape to the round cross-section, as illustrated in Fig. 14. This strongly implies the low shear strength of the film, consistent with the low friction coefficient observed. However, the rolls are a consequence of this behaviour and not the reason – there has never been any evidence that the formation of the roll-like wear debris reduces wear or friction in itself [16,24].

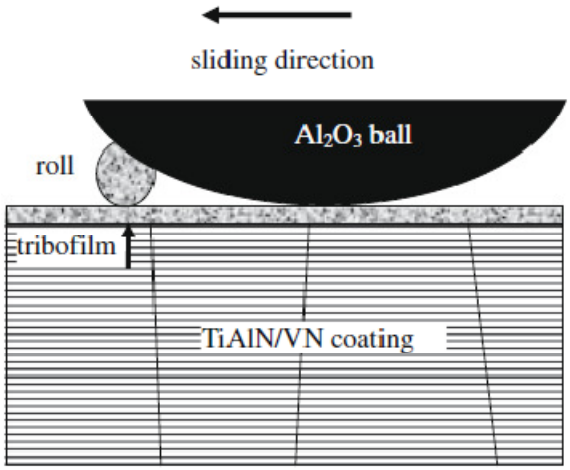

Fig. 14. A low shear tribofilm consisting of Al hydroxides and/or amorphous oxynitride formed between TiAlN/VN hard coating and alumina counterface resulted in excellent tribological properties and extremely low friction. The schematic diagram shows the formation of a roll-like wear debris particle from the tribofilm.

At 25 ^{0}C, the friction coefficient of 0.53 measured in the current work for the TiAlN/VN tests against Al_2O_3 is significantly lower than the values of 0.8–1.0 found for TiAlN/CrN [2] against the same counterface material, using the same test rig. It is also much less than the values of 1.0–1.5 for a similar TiAlN coating worn against alumina (with Al2TiO5 as the major wear debris) [25]. In contrast, ball-on-disc dry sliding tests of VN coatings against Al2O3 [9] exhibited a friction coefficient of 0.45 at 25 ^{0}C, similar to that in the current work for TiAlN/VN. This strongly implies that the VN has inherently lower friction than the CrN at room temperature, and that the alternating layers of TiAlN in the TiAlN/VN did not increase friction significantly. As discussed above, the observed friction coefficient appears to be controlled by the presence of a thin, hydrated amorphous layer, and not by the presence of crystalline Magne´li type phases. Thus, the presence of vanadium even in an amorphous film had a significant effect on friction. The progressive oxidation detected by the EELS study (Fig. 9) from the coating through the tribofilm to the loose wear particles appeared to be associated with the vanadium, as V L_2/L_3 ratio changed, while the Ti L_2/L_3 ratio did not change significantly. Unfortunately, the Al K edge could not be obtained in the same spectrum, given the large difference in energy loss. Nevertheless, it remains far from clear why the addition of vanadium makes such a difference to the friction.

At 300^{0}C, the friction coefficient of the TiAlN/VN had increased appreciably to around 1.0. This is much higher than reported by Fateh et al. [8], who observed a value of 0.5 for VN tested at 300 ^{0}C. In contrast, Pfluger et al. [26] observed a value of 1.5 at 400 ^{0}C for TiAlN deposited by the same method used in the current work. Thus, assuming friction coefficient of TiAlN at 400 ^{0}C is similar to 300 ^{0}C, the friction observed for TiAlN/VN (V: 55.2 at.%) here of 1.0 appears to be mid-way between that for VN and TiAlN, implying a simple law of mixtures, 1.5 x 44.8% + 0.5 x 55.2% = 0.95. However, in the current work, there was clear deformation of the substrate, which resulted in cracking of the coating (Fig. 10). Such deformation may well have contributed to the friction coefficient observed, making comparisons with other reported work less valid.

4.2. Friction behaviour at 635 ^{0}C

The friction observed at 635 ^{0}C was 0.46. This compares with the observations of Fateh et al. [8] who looked at VN and measured values of 0.25 at 700 ^{0}C and 0.34 at 600 ^{0}C. Thus, the current results indicate that the TiAlN component of the coating had increased the friction coefficient observed compared to the value expected for the VN component.

The outer worn surface had a nanocrystalline structure, comprised predominantly of V_2O_5 and possibly other Magne ´li phases, such as VO_2. Below this there was a layer of TiO_2 interspersed by $AlVO_4$ particles. This is consistent with the static oxidation studies that showed the V_2O_5 dominant outer surface on top of $AlVO_4$ and TiO_2 particles [10]. The present observations are also consistent with the findings of Gassner et al. [7] and Fateh et al. [8], who observed VO_2 and possibly V_6O_{13} as well as V_2O_5. In any event, it is clear that, as expected, the low friction is promoted by the outer V_2O_5 layer, which provides some mechanical support as a result of the compacted nanocrystalline nature (often referred to as a glaze layer). Interestingly, there was little evidence of preferred orientation within this layer; rather, the layer had a largely random orientation. However, the absence of a texture at a worn surface is a relatively common observation [27].

While much has been written about the low friction of the V bearing coatings at high temperature, the wear rate at 635 ^{0}C was substantially higher than at room temperature (by a factor of around 40), mainly attributed to the porous oxide scale, which underwent a significant volume expansion, e.g. five times from VN to V_2O_5 on formation (molecular volume VN: 10.7 cm^3, V_2O_5: 54.0 cm^3, TiN: 11.8 cm^3 and TiO_2:18.8 cm^3 [10]). The wear rate is perhaps not surprising, and comparable with a value of 13.1 x 10^{-15} m^3 N^{-1} m^{-1} for (VTi)N coatings against Al_2O_3 at 650 ^{0}C, reported by Ouyang et al. [28]. It is clear that the operating conditions for such coatings in commercial practice would have to be carefully selected so as to avoid the high friction at 300 ^{0}C and the high wear at >600 ^{0}C.

5. Conclusions

1) The friction coefficient exhibited by the coating sliding against alumina was 0.53 at 25 ^{0}C, increased to 1.03 at 300 ^{0}C, and decreased to 0.46 at 635 ^{0}C.
2) The low friction 635 ^{0}C was attributed to the formation of a V_2O_5 "glaze layer" on the oxide surface. This layer comprised a nanoscale polycrystalline structure, with no obvious preferred crystallographic orientation. There was no strong evidence of other vanadium-based oxides in the layer, and the Ti and Al bearing oxides were present below the V_2O_5 dominant surface layer.
3) At 25 ^{0}C and 300 ^{0}C the worn surface comprised a thin (<50 nm) amorphous tribolayer, with no evidence of crystalline Magne´li phases. At both temperatures, the Ti, Al and V content of the tribofilm was essentially the same as the coating, but the nitrogen had been partially replaced by oxygen, i.e. (TiAl-V)O_xN_y. The oxygen level was higher in loose wear debris compared to the tribofilm on the surface.
4) The only differences between the tribofilms at 25 ^{0}C and 300 ^{0}C that could explain the substantial difference in friction was that the tribofilm was hydrated at 25 ^{0}C but not at 300 ^{0}C. The tribofilm at 300 ^{0}C was thicker than at room temperature, but this may have been a sampling error.
5) Surface roll-like wear debris, observed at 25 ^{0}C, but not at higher temperatures, were shown to have the same composition and amorphous structure as the tribofilm. The absence of substructure suggested that the roll formed from displacement from the tribofilm, followed by viscous flow to minimize surface energy.
6) High friction at 300 ^{0}C was also partly attributed to plastic deformation of the substrate, which resulted in through-thickness cracking of the coating.

Acknowledgements

The authors would like to acknowledge the funding of this work by the UK Engineering and Physical Sciences Research Council (EPSRC).

References

[1] Münz W-D. J Vac Sci Technol 1986;4A:2717.
[2] Münz W-D, Lewis DB, PEh Hovsepian, Scho¨njahn C, Ehisarian A, Smith IJ. Surf Eng 2001;17:15.
[3] Constable CP, Yarwood J, PEh Hovsepian, Donohue LA, Lewis DB, Münz W-D. J Vac Sci Technol 2000;18A:1681.
[4] Interntional Chemical Safety Cards, ICSC:0596.
[5] Mayrhofer PH, Hovsepian PEh, Mitterer C, Münz W-D. Surf Coat Technol 2004;177–178:341.
[6] Kutschej K, Mayrhofer PH, Kathrein M, Polcik P, Mitterer C. Surf Coat Technol 2004;188–189:358.
[7] Gassner G, Mayrhofer PH, Kutschej K, Mitterer C, Katherein M. Tribol Lett 2004;17:751.
[8] Fateh N, Fontalvo GA, Gassner G, Mitterer C. Wear 2007;262:1152.
[9] Fateh N, Fontalvo GA, Gassner G, Mitterer C. Tribol Lett 2007;28:1.
[10] Zhou Z, Rainforth WM, Rodenburg C, Hyatt NC, Lewis DB,Hovsepian PEh. Metall Mater Trans 2007;38A:2464.
[11] Godet M. Wear 1984;100:437.
[12] Bajwa S, Rainforth WM, Lee WE. Wear 2005;259:553.
[13] Fischer TE, Tomizawa H. Wear 1985;105:29.
[14] Dong X, Jahanmir S, Hsu S. J Am Ceram Soc 1991;74(5):1036.
[15] Eun KY, Lee K-R, Yoon E-S, Kong H. Surf Coat Technol 1996;86–87:569.
[16] Fischer TE, Tomizawa H. Wear 2000;245:53.
[17] Münz W-D, Smith IJ, Lewis DB, Creasey S. Vacuum 1997;48:473.
[18] Burcham LJ, Deo G, Gao X, Wachs IE. Top Catal 2000;11/12:85.
[19] Luo Q, Zhou Z, Rainforth WM, Hovsepian PEh. Tribol Lett 2006;24:171.
[20] Hofer F, Warbichler P, Scott A, Brydson R, Galesic I, Kolbesen B. J Microsc 2001;204:166.
[21] Binner J, Zhang Y. Ceram Int 2005;31:469.
[22] Sato T, Haryu K, Endo T, Shimada M. J Mater Sci 1987;22:2277.
[23] Krnel K, Drazic G, Kosmac T. J Mater Res 2004;19:1157.
[24] Zhou Z, Rainforth WM, Tan CC, Zeng P, Ojeda JJ, Romero-Gonzalez M, Hovsepian PEh. Wear 2007;263:1328.
[25] Vancoille E, Celis JP, Roos JR. Wear 1993;165:41.
[26] Pflu¨ger E, Schro¨er A, Voumard P, Donohue L, Münz W-D. Surf Coat Technol 1999;115:17.
[27] Rainforth WM. Wear 2000;245:162.
[28] Ouyang JH, Murakamib T, Sasaki S. Wear 2007;263:1347.